KOÇ UNIVERSITY
COLLEGE OF ENGINEERING

MECH 425-525

Mechanics of Microsensors

Project no: #3

Project title:

Force Measurement In nN Range

Name: Feras Kiki

Submission Date: 06/06/2023

Methodology:

The piezo-resistive behaviour of SNWs happens when mechanical stress breaks the cubic symmetry of Si which changes the electronic band structure of the Si crystal. The piezo-resistive coefficient tensor relates the applied stress to the change in the resistivity of Si. For the case of uniaxial stress, this relationship reduces to:

$$\frac{\Delta\rho}{\rho} = \pi_{eff}\,\sigma = \pi_{eff}\,E\,\varepsilon$$

Where ρ is the resistivity, π is the effective piezo-resistive coefficient, σ is the applied normal stress, E is Young's modulus in the loading direction and ε is the strain. To determine the value of π, both the loading direction, crystallographic orientation and doping type and concentration must be taken into consideration.

Table 2. reports the values for both p-type and n-type Si.

The corresponding change in the resistance is:

$$\frac{\Delta R}{R} = (1 + 2\nu) + \frac{\Delta\rho}{\rho}$$

Where ν is Poisson's ratio. Since $\frac{\Delta\rho}{\rho}$ can be two orders of magnitude larger than

$(1 + 2\nu)$, then the above equation can be written as:

$$\frac{\boldsymbol{\Delta R}}{\boldsymbol{R}} = \frac{\boldsymbol{\Delta\rho}}{\boldsymbol{\rho}} = \boldsymbol{\pi_{eff}\,E_{eff}}\,\varepsilon \qquad (1)$$

The sensitivity of the force sensor is expressed in terms of the non-dimensional gauge factor G as:

$$\boldsymbol{G = \frac{\frac{\Delta R}{R}}{\varepsilon} = \pi_{eff}\,E_{eff}} \qquad (2)$$

The higher the gauge factor, the larger is the change in resistance of the SNW with applied stress.

For a uniaxial stress state, $\sigma = E\varepsilon$ or $\frac{F}{2A} = E\varepsilon$. Hence, we can re-write the Equation 2 as

$$\varepsilon = \frac{F}{2AE} = \frac{\Delta R}{R}\frac{1}{G}$$

And In terms of the force,

$$\boldsymbol{\Delta F = \frac{2AE}{G}\,\frac{\Delta R}{R}} \qquad (3)$$

This equation defines another important parameter that characterizes the performance of the force sensor which is the resolution. The force resolution is defined as the smallest change in the force that can be detected given the measurements tool available.

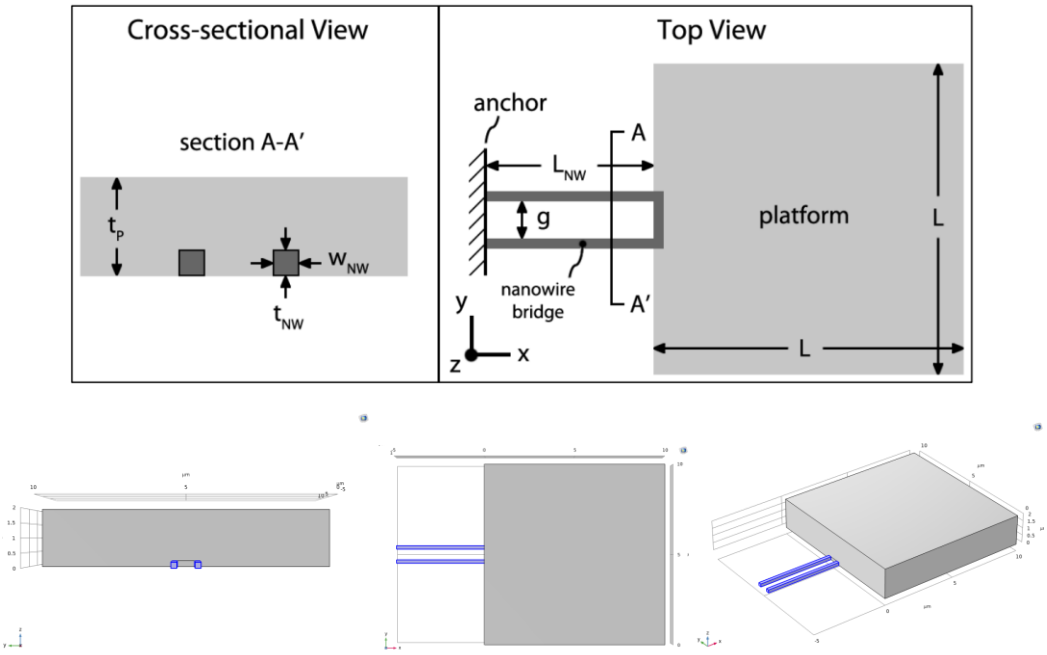

1 Schematic of the sensor structure to be used in questions 1, 2, and 3.

Table 1: Values of relevant parameters for questions 1, 2, and 3.

Description	Symbol	Value
nanowire gauge length	L_{NW}	5 µm
nanowire thickness	t_{NW}	200 nm
nanowire width	W_{NW}	200 nm
gap between nanowires	G	1 µm
platform side length	L	10 µm
platform thickness	t_P	2 µm
effective elastic modulus of silicon along <100> directions	$E_{<100>}$	130 GPa
effective elastic modulus of silicon along <110> directions	$E_{<110>}$	169 GPa
longitudinal piezoresistive coefficient along <100> directions	$(\pi_L)_{<100>}$	π_{11}
longitudinal piezoresistive coefficient along <110> directions	$(\pi_L)_{<110>}$	$(\pi_{11}\ \pi_{12}\ \pi_{44})/2$
piezoresistive coefficients for p-type single crystalline silicon	$(\pi_{11})_p$	6.6×10^{-11} Pa^{-1}
	$(\pi_{12})_p$	-1.1×10^{-11} Pa^{-1}
	$(\pi_{44})_p$	138.1×10^{-11} Pa^{-1}
piezoresistive coefficients for n-type single crystalline silicon	$(\pi_{11})_n$	-102.2×10^{-11} Pa^{-1}
	$(\pi_{12})_n$	53.4×10^{-11} Pa^{-1}
	$(\pi_{44})_n$	-13.6×10^{-11} Pa^{-1}

Results:

The Solid Mechanics and Electric Current Module of COMSOL Multiphysics were used to model the piezo-resistive bridge. A 100nN Force is applied to the platform in the x-direction while the free ends of the bridge are anchored. Analytic and numeric results are shown in Table 2.

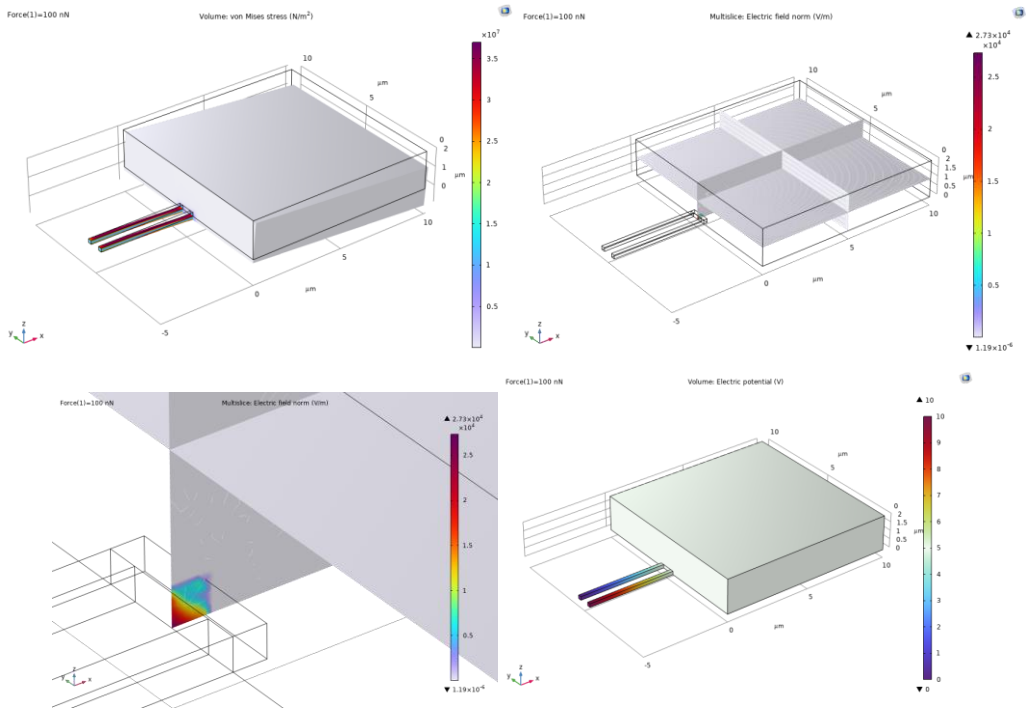

Figure 2 Results plots

Table 2 Results

	p-type doped silicon	n-type doped silicon
<100> orientation	G_{FEM} = 8.50 $G_{analytical}$ = 8.58 difference = 0.009%	G_{FEM} = -136.78 $G_{analytical}$ = -132.86 difference = 0.029%
<110> orientation	G_{FEM} = 121.75 $G_{analytical}$ = 121.34 difference = 0.003%	G_{FEM} = - 51.85 $G_{analytical}$ = -52.73 difference = 0.017%

Table 2 provides a detailed comparison between the numerical (Finite Element Method, FEM) and analytical calculations of the gauge factor (G), a critical non-dimensional parameter that characterizes the sensitivity of the force sensor, for both p-type and n-type doped silicon under two crystal orientations: <100> and <110>. For the p-type doped silicon in the <100> orientation, the numerically obtained gauge factor (G_{FEM}) was found to be 8.50, which closely aligns with the analytically calculated value ($G_{analytical}$) of 8.58. The minor discrepancy between these results amounts to a difference of only 0.009%, affirming the high accuracy of the numerical model in this case. A similar consistency between numerical and analytical results was found for the <110> orientation in the p-type doped silicon, with a marginal difference of 0.003%.

In contrast, the n-type doped silicon showed a greater difference between numerical and analytical values of the gauge factor. For the <100> orientation, the numerical and analytical results were -136.78 and -132.86, respectively, giving a larger difference of 0.029%. For the <110> orientation, the difference was less, but still significant, at 0.017%. These findings illustrate the reliability of the numerical model, especially for p-type doped silicon, while showing some discrepancies for the n-type doped silicon. However, it should be emphasized that these discrepancies are relatively small and might be due to inherent approximations involved in the FEM simulations or in the assumptions made in the analytical model. These results are paramount for validating the numerical model and for understanding the relative sensitivities of force sensors based on different dopant types and crystal orientations of silicon. The comparison between FEM and analytical results provides a robust benchmark for future studies and for the optimization of force sensors using piezoresistive silicon nanowire bridges.

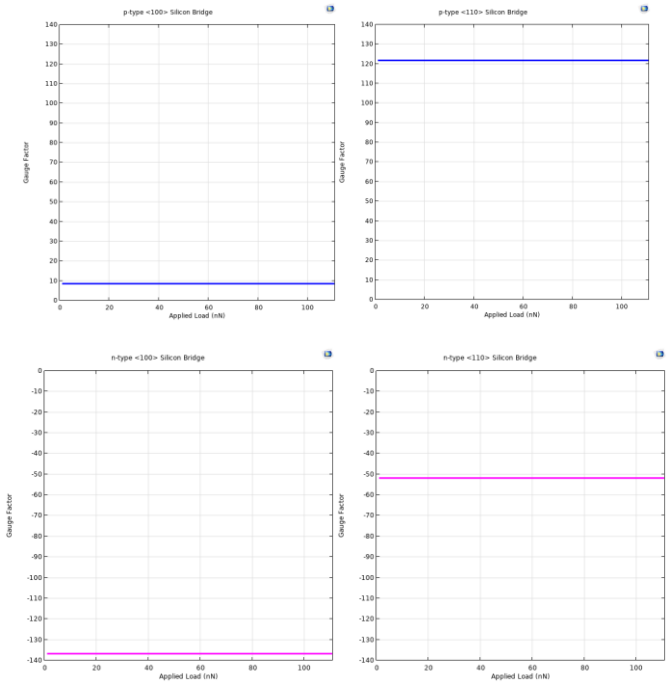

Figure 3 (top) Gauge factor value for p-type, (bottom) Gauge factor value for n-type

Equation 2 presents the gauge factor (G), a dimensionless variable that expresses the sensitivity of the force sensor. The gauge factor only depends on the properties of the material and its stress state. Importantly, it does not depend on the magnitude of the applied load, which is a crucial aspect of the gauge factor's characteristics. This property of the gauge factor has been confirmed using COMSOL Multiphysics, a software platform for physics-based modeling and simulation. Nevertheless, it's important to keep in mind that as the load increases significantly, the gauge factor might change. This is because a high load can induce substantial bending moments, which may invalidate the assumption of a uniaxial stress state. Moreover, larger strains may substantially degrade the electrical properties of the Silicon Nanowires (SNWs). Therefore, when dealing with high loads, different material models other than linear elasticity might need to be considered. Thus, gauge factor is independent of the applied load magnitude under certain conditions. However, when these conditions are significantly altered - for instance, through the application of a large load leading to high strains and substantial bending moments - the gauge factor might change and different material models may be necessary.

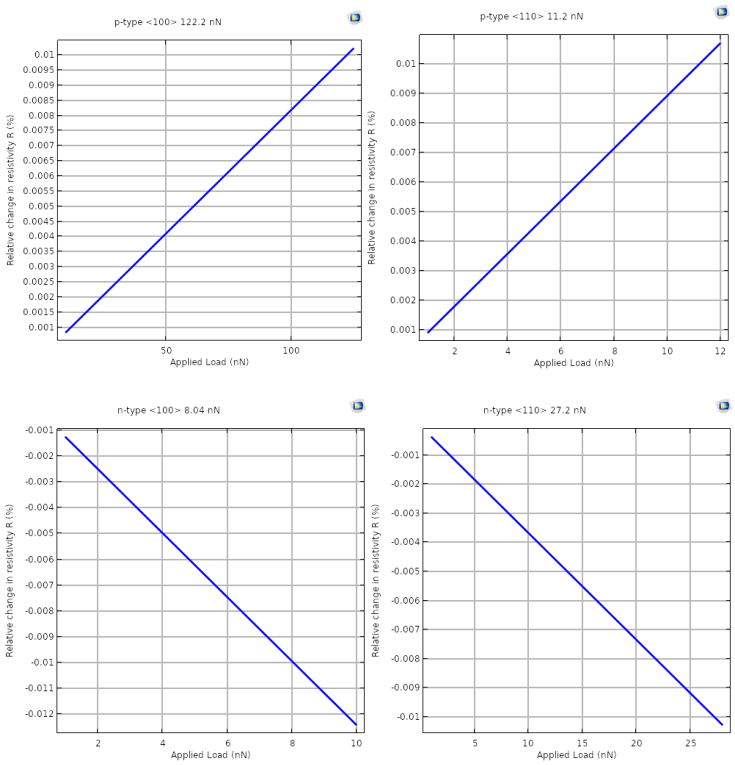

Figure 4 Resolution for 0.01% change in relative R

Based on the force resolution values for each combination of orientation and dopant type, we can infer several insights about the sensitivity and potential application of each setup. The force resolution of a nanowire bridge essentially refers to the smallest detectable change in force by the system. A lower force resolution indicates a higher sensitivity to changes in force, meaning the system can accurately detect and respond to smaller changes. From the given values, we see that the n-type <100> silicon nanowire offers the lowest force resolution (8.04 nN), indicating that it has the highest sensitivity among the four configurations. This setup would be the most suitable for applications where a high level of precision is required, such as in microscale mechanical testing or in sensitive nanoscale force sensors.

On the other hand, the p-type <100> silicon nanowire has the highest force resolution (122.2 nN), indicating the lowest sensitivity. This configuration might be more suitable for applications where large forces are expected, or where high sensitivity is not necessary. Despite its lower sensitivity, it might offer other advantages, such as robustness to noise or a higher maximum allowable force. The force resolution for the p-type <110> and n-type <110> are between these two extremes, and these configurations may be suitable for a range of applications depending on the specific force range and sensitivity requirements. Furthermore, it's worth noting that the orientation of the silicon nanowire also plays a significant role in its force resolution. The <110> orientation shows better force resolution than the <100> orientation for both p-type and n-type dopants. This indicates that in addition to the type of dopant, the crystallographic orientation of the silicon nanowire significantly impacts its piezoresistive properties, and therefore its force sensing capabilities.

When designing a nanoscale force sensing system using piezoresistive silicon nanowires, careful consideration must be given to both the dopant type and the crystallographic orientation of the nanowire.

Different configurations offer different trade-offs between sensitivity, force range, and potentially other factors such as robustness to noise or environmental conditions, making each configuration suitable for different applications.

Part 2:

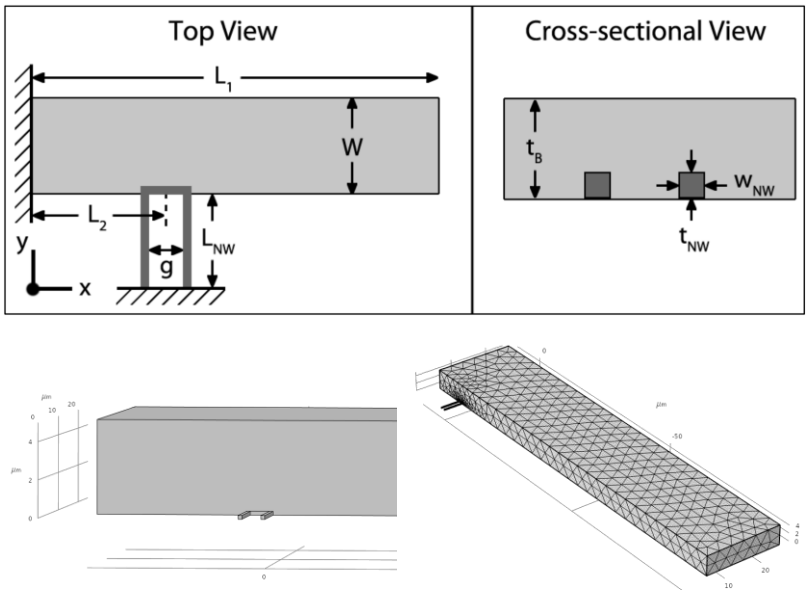

Figure 5 Schematic of the sensor structure to be used in question 4.

Table 3 Values of relevant parameters for question 4

Description	Symbol	Value
nanowire gauge length	L_{NW}	5 µm
nanowire thickness	t_{NW}	200 nm
nanowire width	w_{NW}	200 nm
gap between nanowires	g	1 µm
cantilever beam length	L_1	100 µm
cantilever beam width	W	5 µm ≤ W ≤ 20 µm
cantilever beam thickness	t_p	5 µm
location of the center line of nanowire bridge	L_2	10 µm ≤ W ≤ 90 µm

The sensor's geometry has been meticulously optimized using COMSOL Multiphysics to achieve an exceptional force resolution of 5nN or less. This assumes the availability of an electrical measurement method capable of resolving a relative change in resistance of 0.01%.

Initially, it may seem logical to position the SNW bridge near the loaded tip of the cantilever, where it would experience the most significant displacement, resulting in a substantial change in resistance. However, thorough simulations, as depicted in Figure 6, demonstrate that this approach is not effective. Placing the bridge in that location leads to substantial bending, ultimately reducing the sensitivity of the sensor.

Consequently, a systematic parametric sweep becomes necessary to determine the optimal position for the SNW bridge. The dependence on the bridge's position is graphically depicted in Figure 7, revealing that the optimal value for parameter L2 is 25.3 µm.

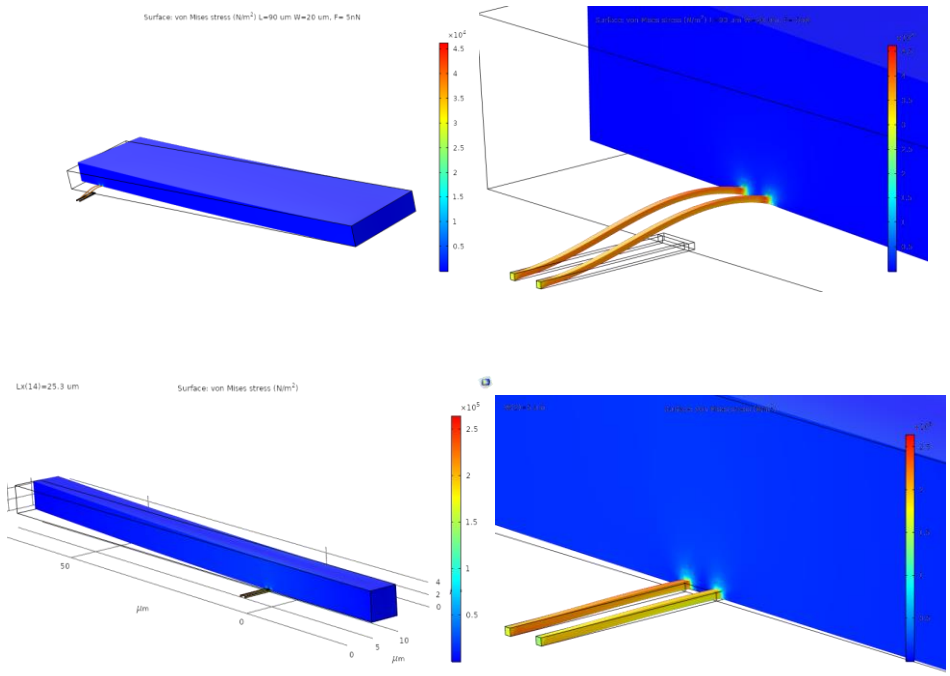

Figure 6 (top) Initial parameters, (bottom) optimized

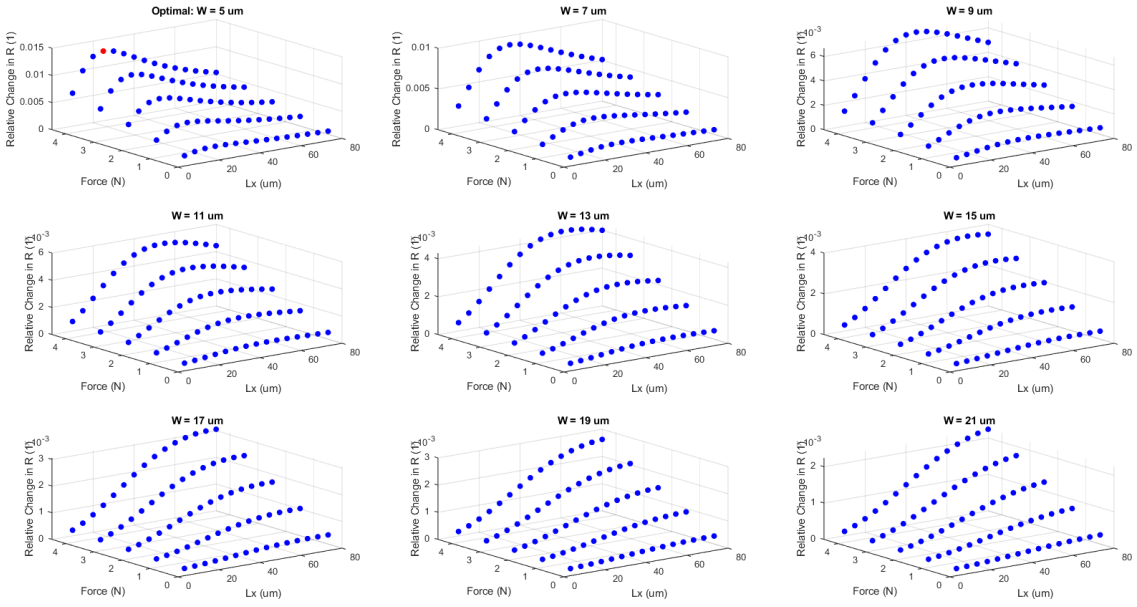

Figure 7 all values sweep for W, L2, Force

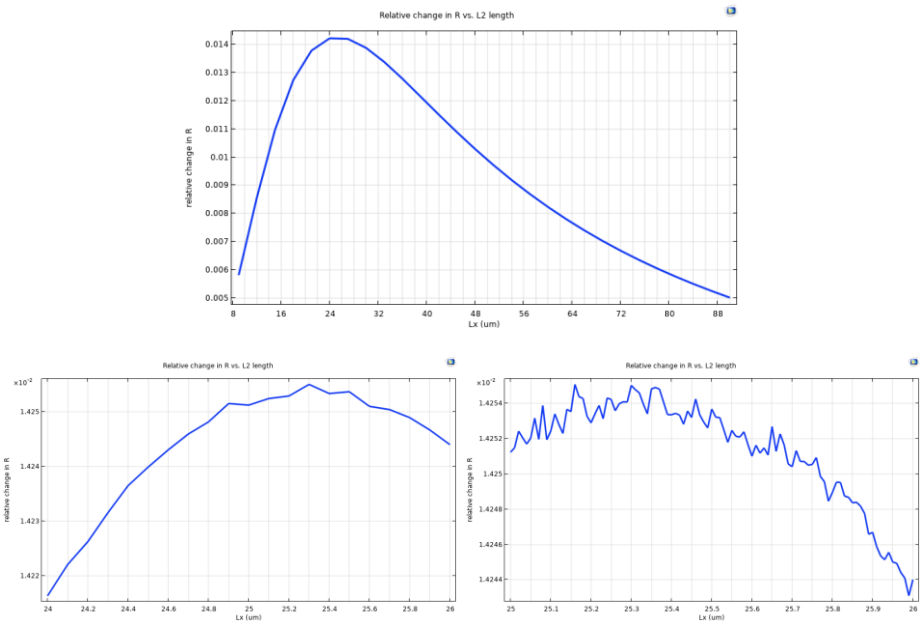

Figure 8 The effect of L2 distance on relative change in resistance showing that optimal value is near 25.3 µm. (top) L2 sweep from 10-90 µm, (bottom) precise sweeps to show optimal value

A comprehensive sweep across a broad range of variable values was performed within the COMSOL Multiphysics platform. This process, a cornerstone of simulation and modeling, enabled the exploration of how the system behaves under various conditions. A defined set of values for each variable was assigned for the sweep. COMSOL then computed the outcomes for each variable combination, generating an extensive set of results that encapsulated the model's behavior under different circumstances. The importance of sweeping is manifold. It offers an understanding of how sensitive the model is to changes in input variables, and aids in identifying any areas of particular interest or concern. For example, if certain variable combinations give rise to especially high or low gauge factors, these areas might necessitate further exploration. Optimization is another crucial benefit conferred by sweeping. By surveying the entire landscape of potential variable combinations, it becomes possible to discern the specific values that lead to optimal performance based on predefined criteria. In this study, sweeping was employed to home in on the optimal value. After identifying a preliminary optimal range via the sweeping process, a narrower, more focused exploration within that region was conducted to pinpoint the precise optimal value.

An iterative approach of a broad initial sweep followed by a narrower, more focused search (Figure 8) is a highly efficient strategy for optimization. This method ensures that the search does not prematurely converge on a local optimum while facilitating the discovery of the best possible solution in an efficient manner. In this study, despite observing a trend in the variables as depicted in the Figure 7, sweeping across a broad range was still carried out. This approach offered several advantages. Firstly, by sweeping broadly, the overall trends and patterns within the data were confirmed, reinforcing the reliability of the findings. Secondly, by continuing to sweep, a more nuanced understanding of the variable interactions was obtained, adding depth to the interpretation of the results.

One alternative to sweeping across all variable combinations is to utilize a guided or smart search strategy, such as a gradient-based optimization method or other algorithms. These methods use heuristics to explore the variable space more efficiently, focusing on areas of the space that are most likely to yield

improved results. However, these approaches require more complex implementation and may miss certain areas of the space that could be relevant to the problem at hand. The sweeping method used in this study, while perhaps more computationally intensive, provides a more thorough and reliable exploration of the variable space.

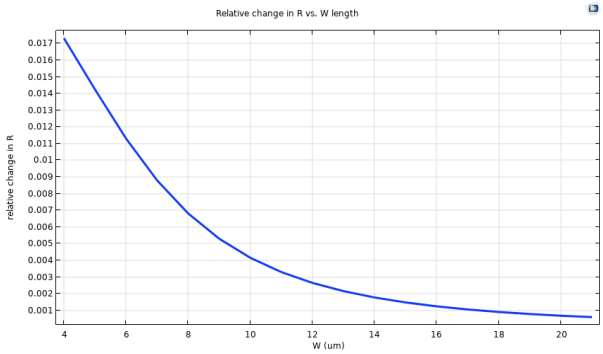

Figure 9 Effect of W on relative change in resistance

We observe from the Figure 9 above regarding effect of W on the system that lower values of the width, W, yield a significantly higher sensitivity. This finding aligns with established principles of mechanics concerning the behavior of cantilever beams. As the width (W) of a cantilever beam increases, the beam's resistance to an applied load also increases. In other words, a wider beam is less likely to deform significantly under the same load as a narrower beam, thereby displaying a lower sensitivity. The reason behind this phenomenon lies in the geometry of the beam. The resistance of a beam to bending is proportional to its moment of inertia, which, for a rectangular cross-section, is proportional to the width times the cube of the depth. Hence, increasing the width increases the moment of inertia dramatically, leading to a significantly higher resistance to bending. In the context of the piezoresistive silicon nanowire bridge studied here, a smaller width (W) corresponds to a higher relative change in resistance under an applied load. Thus, the sensitivity of the device (as measured by the gauge factor) is greater for smaller widths. However, while increased sensitivity is generally desirable, it's important to consider the trade-offs. For instance, a smaller width might also correspond to a reduced load-bearing capacity or a higher likelihood of structural failure under high loads. As such, the optimal width for a specific application would need to be determined by balancing the need or high sensitivity with other practical considerations such as durability, stability, and load-bearing requirements.

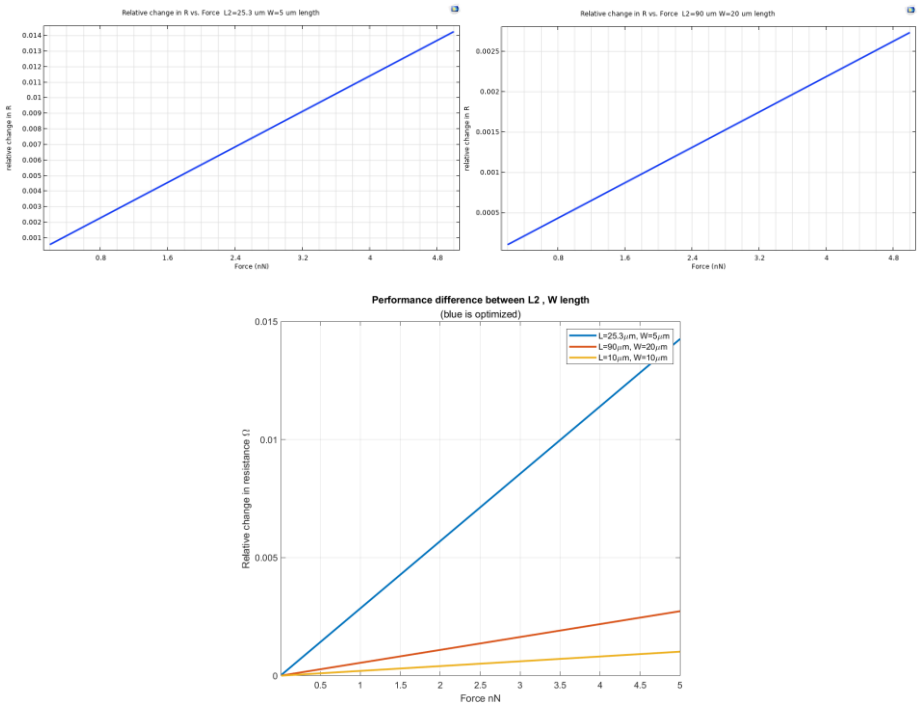

Figure 10 different resolutions depending on L2, W parameters values
(top) single plots, (bottom) combined plots to show the difference

Figure 10 above serves as a comprehensive representation of the dependency of sensitivity on the two key geometric parameters of the cantilever beam: width (W) and length (L2). It allows us to visualize the complex interplay between these parameters and their collective effect on the sensitivity of the piezoresistive silicon nanowire bridge. The top portion of Figure 10 showcases individual plots for different combinations of W and L2. These individual plots provide specific insights into how each pair of parameters affects the sensitivity of the device. In each plot, the relative change in resistance in response to an applied load is displayed, which directly corresponds to the sensitivity of the device. The bottom portion of the Figure presents these individual results collectively in a combined plot. This allows for a comparison between the sensitivities achieved with different W and L2 combinations. The combined plot helps illustrate the differential effects of these parameters and highlights how certain combinations can result in higher sensitivity. From these graphical representations, it can be inferred that the chosen values for W and L2 parameters provide the highest change in resistance for a given applied load. This implies that these selected values offer the greatest sensitivity, making them highly suitable for applications that require a highly responsive force sensor.

However, while these chosen parameter values yield the highest sensitivity, it's essential to consider other aspects such as structural stability and durability. These additional considerations might necessitate adjustments to the parameters to achieve an optimal balance between sensitivity and the physical robustness of the device.

Part 3: Literature Review for doping concentration

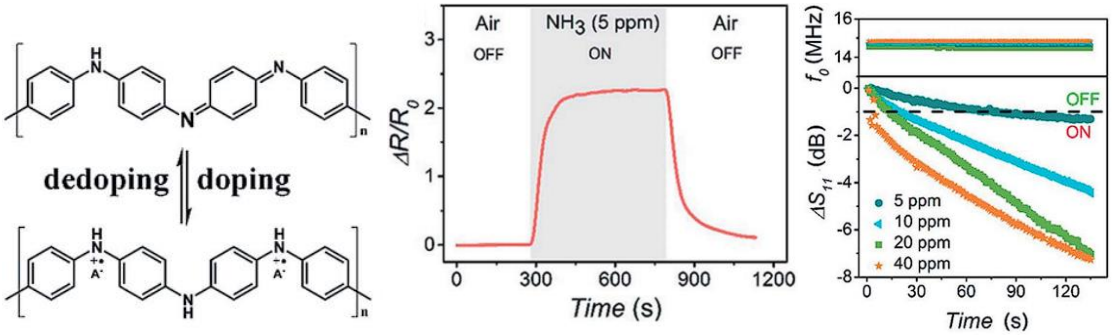

Figure 11 [2]
(left) The reversible doping/dedoping process of PAni results in the conversion between conductors and insulators.
(middle) The resistance responses of PAni to ammonia and putrescine.
(right) The real-time responses to different concentrations of ammonia of the PAnimodified NFC tag in terms of the reflection coefficient and resonant frequency.

The paper discusses the role of dopant concentration in conductive polymer hydrogels (CPHs) and their applications in sensor technologies. The authors highlight the unique combination of hydrogels and organic conductors, which makes CPHs a promising platform for various sensor technologies [2].

Effect of Dopant Concentration: The authors mention that doping is the main process to improve the electrical properties of CPHs. Doping introduces charge carriers of a relatively higher density into the polymer structures, which are able to move along the interconnected 3D network. The choice of dopant, doping strength, and doping level determine the conductivity of CPHs. The conductivity of CPHs can be tuned over a wide range by controlling its doping level. Furthermore, the doping-induced nanostructures are able to enhance the interchain charge transport [2].

Advantages: High dopant concentration can lead to high conductivity, which is beneficial for achieving excellent sensitivity and stability in CPH-based sensors. The paper also mentions that the doping process is reversible, which is favorable for introducing novel sensing functions and has applications in chemical sensors. The authors also discuss that the high doping level and conjugated polymer chains, along with the continuous interconnected network, play an important role in facilitating electron transport [2].

Disadvantages: The paper mentions that nonvolatile dopants are difficult to remove, especially in the high-temperature range. This could potentially limit the versatility of the material in certain applications

The paper discusses various applications of CPHs in sensor technologies, including pressure sensors, biosensors, and gas sensors. The authors highlight that the key function of CPH-based sensors is to respond to external stimuli with a corresponding change in the electrical signal output.

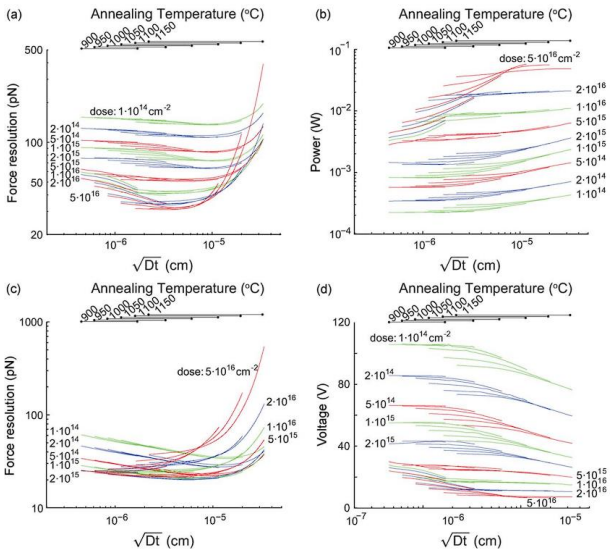

Figure 12 [3] Simulated force resolution of a 2000-µm-long, 30-µm-wide, and 7- µm-thick ion-implanted cantilever with a 350-µm-long, 15-µm-wide, and 50-keV boron-implanted piezoresistor.

This study investigated the effects of various parameters on the performance of cantilevers, specifically focusing on the role of the dopant. It was discovered that the optimal performance of a typical cantilever, under a constant power of 25mW, is achieved with a moderate dose of dopant and a diffusion length of 5*10^-6 cm [3]. A larger dopant dose improved force resolution in the case of constant bias voltage, but an intermediate dose was optimal for constant power dissipation. Dopant concentration significantly influences carrier mobility, which, along with the elementary charge, dopant concentration, and longitudinal piezoresistance factor, impacts device performance [3]. The piezoresistance factor was found to be a function of dopant concentration and was modelled using Richter's analytical model. Investigations were carried out to observe how diffusion affects the piezoresistance factor with various annealing conditions. Optimized cantilevers were compared with non-optimal designs, and it was noted that the thickness and length of the cantilevers, the piezoresistor width, and junction depth were all crucial determinants of the force resolution. The optimal cantilevers achieved force resolutions of 72.5 and 69.8 pN, which were close to the analytically predicted resolution of 68.1 pN. The best force resolution, however, was achieved with a cantilever fabricated with a 2*10^15-cm^−2 dose and 4.8*10^−6-cm diffusion length. The study emphasized that while the optimization technique generated optimal cantilever designs with constraints on bias voltage and power dissipation, a simple optimization technique applied to an ion-implanted cantilever could lead to high force resolution due to low dopant concentration and long piezoresistor length. The study concluded that the analytical model closely predicted the experimental force resolution, with the experimental results being in good alignment with the model. However, certain factors such as the cantilever air trench, interconnects, and contact pads caused slight variations in the predicted and actual outcomes[3].

Table 4 Voc: the open circuit voltage; Isc: the short circuit current 22 [4]

Film thickness (nm)	V_{oc} [mV]	I_{sc} [nA]	Carrier concentration N [cm−3]
1000	9.8	-1940	1.4~6.2 x10^{18}
380	8.5	-1057	2.5~10 x 10^{18}

280	9.6	-670	1.5~6.8 ×10^{18}
130	9.4	-480	1.5 ~7.0 ×10^{18}

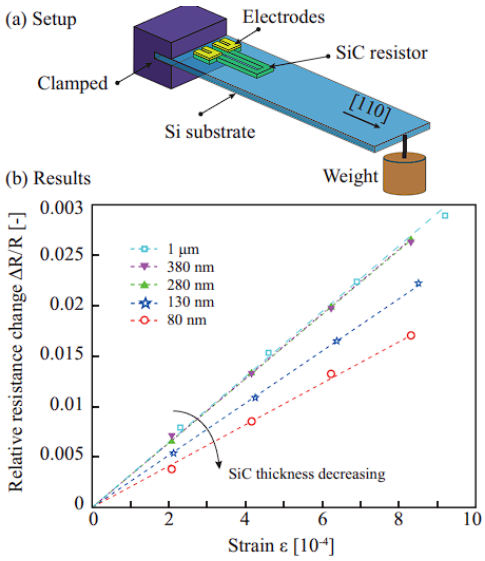

Figure 13 [4] (top) device,
(bottom) The relationship between the relative resistance change of 3C-SiC resistors and applied strain

In this study, the piezoresistive effect of p-type single crystalline 3C-SiC nano thin films, grown by Low Pressure Chemical Vapor Deposition (LPCVD), is characterized for the first time [4]. The thickness of these films ranged from 80 nm to 1 μm, and the films were grown on Si(100) substrates using a hot-wall LPCVD reactor at 1000°C. Trimethylaluminium was used as the p-type dopant for in situ doping [4]. The fabrication process resulted in SiC/Si strips with different thicknesses that reflect different colors when observed under an optical microscope. The SiC resistors were patterned into a U-shaped structure to study the piezoresistive effect, and aluminum contact pads were added at each end of the resistor. Four terminal resistance measurements were performed to eliminate contact resistance. The hot probe technique was used to characterize the doping type and the carrier concentration of the 3C-SiC films. It was found that all the SiC films were p-type semiconductors, and the carrier concentrations were in the range of approximately 1.4 ~ 10 × 10^18 cm^−3. The study also investigated potential issues of current leakage through the SiC/Si junction, confirming that the Si substrate did not contribute to the measured gauge factor. The ratio of the current leakage to the current through the SiC resistor was found to be below 0.5%. Previous studies found that the piezoresistive effect is dominated by the shear piezoresistive coefficient π44, with the [110] orientation possessing the largest gauge factor. Therefore, this study focused on characterizing the longitudinal gauge factor of the [110] direction of the p-type single crystalline 3C-SiC films. The piezoresistive effect of 3C-SiC was measured using the bending method [4]. The strain distribution in the SiC resistor was found to be relatively uniform, matching the strain of the top surface of the Si substrate. The linear relationship between the relative resistance change of the p-type 3C-SiC and the applied tensile strain was also noted [4].

Conclusion:

In this study, we thoroughly explored the behavior of a piezoresistive silicon nanowire bridge under various conditions, using the COMSOL Multiphysics platform to understand the effect of two key

geometric parameters: the width (W) and the length (L2). Our comprehensive variable sweep enabled us to understand the sensitivity of our model to changes in these inputs, and, importantly, it facilitated our identification of the optimal parameter values that led to the highest gauge factor. We found that smaller values of width (W) led to a significantly higher gauge factor, a result that is in line with established principles of mechanics related to cantilever beams. However, we also acknowledged that while high sensitivity is desirable, practical considerations such as durability and stability may impose constraints on how small the width can be. The interplay between width (W) and length (L2) parameters was effectively visualized, revealing a complex yet informative pattern. The chosen optimal values for these parameters provide the highest relative change in resistance for a given load, implying a high sensitivity. This makes the piezoresistive silicon nanowire bridge highly suitable for applications that demand a highly responsive force sensor. However, it is crucial to remember that achieving the highest sensitivity is a balance between optimizing geometric parameters and maintaining the physical robustness of the device. Thus, further research may be directed towards exploring this balance in detail, potentially considering other relevant parameters and their effects on performance. Additionally, real-world testing and validation of the model's predictions will be a critical next step. This research has opened avenues for the development of highly sensitive force sensors, which can find extensive applications in various fields. Further studies building on these findings can lead to even more optimized sensor designs, making significant contributions to the realm of force sensing technology.

References:

[1] P. E. Allain, A. Bosseboeuf, F. Parrain, S. Mâaroufi, P. Coste and A. Walther, "Large range MEMS motion detection using integrated piezo-resistive silicon nanowire," 2012 IEEE 25th International Conference on Micro Electro Mechanical Systems (MEMS), Paris, France, 2012, pp. 1320-1323, doi: 10.1109/MEMSYS.2012.6170401.

[2] Ma Z, Shi W, Yan K, Pan L, Yu G. Doping engineering of conductive polymer hydrogels and their application in advanced sensor technologies. Chem Sci. 2019 May 29;10(25):6232-6244. doi: 10.1039/c9sc02033k. PMID: 31367298; PMCID: PMC6615242.

[3] S. -J. Park, J. C. Doll, A. J. Rastegar and B. L. Pruitt, "Piezoresistive Cantilever Performance—Part II: Optimization," in *Journal of Microelectromechanical Systems*, vol. 19, no. 1, pp. 149-161, Feb. 2010, doi: 10.1109/JMEMS.2009.2036582.

[4] Phan, Hoang-Phuong & Dao, Dzung Viet & Tanner, Philip & Han, Jisheng & Nguyen, Nam-Trung & Dimitrijev, Sima & Walker, Glenn & Wang, Li & Zhu, Yong. (2014). Thickness dependence of piezoresistive effect in p-type single crystalline 3C-SiC nano thin film. J. Mater. Chem. C. 2. 10.1039/C4TC01054J.